

**Article Citation Format**

Bori, I., Uwah, E.J., Bako, S., Okegbile, O.J. & Ayo, S.A. (2022):  
Design and Performance Evaluation of A Portable Solar  
Water Heater  
. Journal of Digital Innovations & Contemporary Research in Science,  
Engineering & Technology. Vol. 10 No. 1. Pp 49-62  
DOI: dx.doi.org/10.22624/AIMS/DIGITAL/V10N1P5

**Article Progress Time Stamps**

Article Type: Research Article  
Manuscript Received: 11<sup>th</sup> Dec, 2021  
Review Type: Blind  
Final Acceptance: 9<sup>th</sup> March, 2022

## Design and Performance Evaluation of a Portable Solar Water Heater

<sup>1\*</sup> Bori, Ige, <sup>2</sup>Uwah, Ebubechukwu Jude, <sup>3</sup>Bako, Sunday, <sup>1</sup>Okegbile, Olawale James & <sup>1</sup>Ayo, Samuel Adinoyi

<sup>1</sup>Department of Mechanical Engineering, Federal University of Technology Minna, Nigeria

<sup>2</sup>Department of Mechanical Engineering, Baze University, Abuja, Nigeria

<sup>3</sup>Department of Mechanical Engineering, Nuhu Bamalli Polytechnic, Zaria, Nigeria

\* **Corresponding Author: E-mail:** ige.bori@futminna.edu.ng

**Phone:** +2349032502267

### ABSTRACT

This paper presents design and performance evaluation of a solar water heater (SWH) using thermosyphon principles, thereby eliminating the use of electric water pump and reducing the cost of the entire system. There are many phenomena encouraging the application of solar water heating technology such as; electric power outage, high fuel price, rapid urbanization, low cost of installations, and governmental intervention. Therefore, there is need to encourage innovation in the field of solar technology. The design of this system was done using relevant equations to obtain the required dimensions of the various components of the system. The materials were selected based on design calculations, machining, availability and material cost. During the testing process, the first three days of testing the highest outlet temperature recorded was 65°C. For the last three days of testing during the dry season, the highest outlet temperature recorded was 79.3 °C. The results showed that the system performs better during the dry season when the irradiance levels are higher. The highest irradiance recorded was 940 W/m<sup>2</sup> on the sixth day of testing. The highest efficiency recorded from the system was 68.19% on the fourth day of testing. It is hereby recommended that, sensor and a flow meter should be installed for determining water level and for easy identification of flow rate.

**Keywords:** Solar Water Heater, Thermosyphon, Design, Development, and Performance Testing

### 1. INTRODUCTION

The need for Solar Water heater (SWH) is increasing daily due to some factors such as; electric power outage, high fuel price, rapid urbanization, low cost of installations, government intervention, and environment-friendly application which acts as a direct replacement to fossil fuels. However, there are many challenges involved in the application of solar technology for domestic and industrial water heating [1]. The utilization of solar collectors to transform radiation into heat energy is the basis of the solar water heating technology. A simple solar water heater consists of a collector, a tank, and the flow channel through which the working fluid is transported.

Considering the epileptic nature of electric power outage in developing countries, the reliance on solar applications for water heating will lead to better reliability of service for hot water needs and will have minimum negative impact on environment pollution. This would reduce the reliance on electric heaters, which have high operational costs and dependent on fossil fuels and problem of electric power outage. Unlike the works done by [2], [3] and [4], this work involved design and performance evaluation of a flat-plate solar water heating system using thermosyphon principle. The application of the thermosyphon principle eliminates the need of an electric pump, thereby reducing the cost of the SWH system. In this system, the storage tank is separated from the solar collector. The solar collector is installed below the storage tank for the thermosyphon effect to work effectively. Natural convection transports this heated water in the collector pipes into the storage tank through the pipes at the top of the collector. Cold water from the tank simultaneously descends to the pipes at the bottom of the solar collector due to its high density, and the cycle continues [5]. The schematic diagram of the thermosyphon solar water heating system is shown in Figure 1.

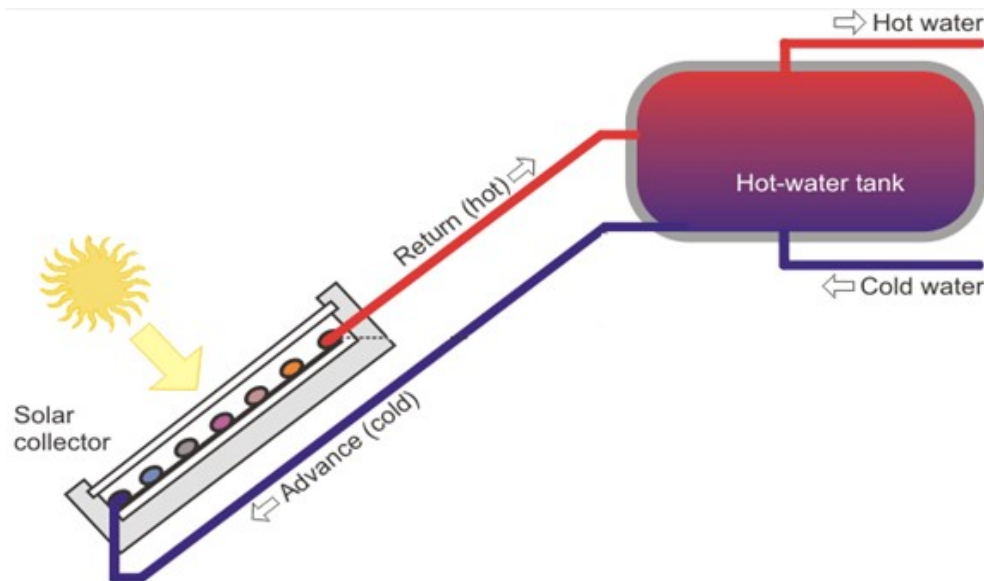


**Figure 1: The Schematic Diagram of a Thermosyphon solar heating system [6]**

The analysis of global solar irradiance over climatic zones in Nigeria for solar energy applications was carried out by [6]. High values of global solar irradiance were observed in the northern regions of the country, compared to the southern regions. However, [7] developed a model that forecasts the solar radiation of Abuja Nigeria, using computer neural networks. It was noted that Abuja has higher solar radiation during equinoxes, with mid-day values exceeding  $600 \text{ W/m}^2$  compared to the mid-day values at solstices, which sometimes dropped below  $500 \text{ W/m}^2$ . For this reason, Abuja was selected as the case study. Abuja, is in the northern part of Nigeria with latitude of  $9.0765^\circ \text{ N}$  and a longitude of  $7.3986^\circ \text{ E}$ .

The angle of inclination made by the absorber of the solar collector with the horizontal is known as the collector tilt angle and is usually denoted by ' $\beta$ ' in most of the literature. Collector tilt angle plays a vital role in the stratification of storage tank of a thermosyphon solar water heating system. It was also noted that the inclination angle should be equivalent to the latitude of a given location [8]. For this reason, this machine is designed to have inclination angle of  $9^\circ$  due to the latitude of Abuja Nigeria..

## 2. MATERIALS AND METHOD

### 2.1 Material selection

The materials selection for this design was based on the design specifications, material availability and cost, material properties, component function and the manufacturing processes involved. While the materials were sourced locally.

### 2.2 Design of the SWH

The key components considered during the design process were the flat-plate collector, the storage tank, and the flow channel. The following assumptions and specifications were considered during the design process:

1. The flow inside the tubes is laminar and uniformly distributed.
2. The radiation incident on the collector was considered to be uniform.
3. The following specifications were taken into consideration;
  - i. Total heating time,  $t$  5 hours
  - ii. Number of flow cycles,  $n$  5
  - iii. Ambient temperature,  $T_i$  22 °C
  - iv. Desired outlet temperature,  $T_o$  70 °C
  - v. Collector efficiency,  $\eta$  58 %
  - vi. Tank diameter to height ratio,  $\frac{H}{d_{st}}$  3

### 2.3 Design process

The daily hot water demand was used to determine the storage tank volume as shown by Equation 1 [10]:

$$V_{st} = 1.2[(P \times HWD)] \quad 1$$

Taking  $\frac{H}{d_{st}} = 3$ , the required storage tank diameter and length was calculated using Equation 2:

$$V_{st} = \frac{\pi d_{st}^2}{4} H \quad 2$$

amount of thermal energy required to heat up a given volume of water is given by (Equation 3):

$$Q_{st} = \frac{m C_w (T_o - T_i)}{3600} \quad 3$$

Since mass is a function of volume and density, Equation 3 can be written as:

$$Q_{st} = \frac{\rho V_{st} C_w (T_o - T_i)}{3600} \quad 4$$

In the course of this research work, it was observed that, June, July, and August have the lowest values of irradiance annually. The use of irradiance values from these three months, enable better performance during other months of the year.

The Efficiency of the collector can be calculated by:

$$\eta = \frac{\text{heat output}}{\text{heat input}} = \frac{Q_{st}}{I A_c} \quad \text{5}$$

Re-arranging Equation 5 to determine the collector area gives:

$$A_c = \frac{Q_{st}}{\eta I} \quad \text{6}$$

The heating time per flow cycle,  $t_n$  is given by:

$$t_n = \frac{t}{n} \times 3600 \quad \text{7}$$

The volumetric flow rate,  $V$  is determined by:

$$\dot{V} = \frac{V_{st}/1000}{t_n} \quad \text{8}$$

For fluid flow, volumetric flow rate ( $V$ ) is expressed as:

$$\dot{V} = A_f U \quad \text{9}$$

Equation 9 can also be expressed in terms of the pipe diameter as:

$$d_p = \sqrt{\frac{4 \dot{V}}{\pi U}} \quad \text{10}$$

For heat transfer across a cylindrical wall, the heat loss is given by:

$$Q_L = \frac{2\pi K N (T_0 - T_1)}{L_n (r_2/r_1)} \quad \text{11}$$

Re-arranging Equation 11 gives:

$$r_2 = r_1 \left[ \frac{2\pi K (T_0 - T_1)}{\varepsilon (Q_L/N)} \right] \quad \text{12}$$

Where  $\frac{Q_L}{N}$  is the heat loss per unit length in W/m.

The heat loss per unit length is given by:

$$\left(\frac{Q_L}{N}\right) 0.125m = X \times \left(\frac{Q_L}{N}\right) 1m \quad 13$$

The thickness of the insulation material X is given by:

$$X = r_2 - r_1 \quad 14$$

### 3. DEVELOPMENT PROCESS

The materials used during the construction process are, Aluminum alloy, aluminum plate , copper pipe, stainless steel and fiber glass insulator, angle metal and black paint. While the manufacturing processes used during the development process were; cutting, rolling, welding, grinding, drilling, hammering, chiseling, and painting. The engineering drawing and the complete fabrication of the solar water heated are shown in the appendix.

### 4. TESTING PROCEDURE

The collector is tilted at an angle of 9° with respect to the horizontal plane. Since Abuja is in the northern hemisphere, the system is directed south wise for the testing. The ambient temperature, the inlet and outlet temperature from the collector were measured every hour from 10 am to 3 pm on three different days. It should be noted that incessant rainfalls prolonged test duration. The flow rate was determined by using a stopwatch and a calibrated container to obtain the volume of flow per minute. This was done repeatedly, and an average value of 0.15 litres /min was gotten.

### 5. RESULTS AND DISCUSSION

The results obtained during the performance evaluation of the SWH are shown in the tables 1, 2, 3, and 4 below. The testing were conducted in two sets on three different days. The first set during the late rainy season and the second set during the dry season. Using the average flow rate of 0.0025 kg/s and the other readings obtained during testing, the system efficiency was calculated using Equation 5 for each set of data.

**Table 1: Readings for the first day of experiments**

| Time (h) | Ambient Temp (°C) | Inlet Temp (°C) | Outlet Temp (°C) | Irradiance W/m <sup>2</sup> | Efficiency (%) |
|----------|-------------------|-----------------|------------------|-----------------------------|----------------|
| 10:00    | 25.00             | 25.00           | 27.00            | 565                         | 4.89           |
| 11:00    | 27.00             | 30.00           | 30.50            | 603                         | 1.15           |
| 12:00    | 28.00             | 30.00           | 31.10            | 704                         | 2.16           |
| 13:00    | 28.00             | 30.00           | 50.00            | 826                         | 33.45          |
| 14:00    | 28.00             | 32.00           | 65.00            | 681                         | 66.95          |

Figure 2(a) shows a significant increase in the irradiance levels compared to the first three days of the testing. It was observed that the irradiance peaks at 12pm unlike the values from day one to three. The outlet temperature is also at peaks at 12pm and reached higher values compared to results for the first three days. From Figure 2(b), it is noticeable that the efficiency and the outlet temperature have a close relationship as they peak at the same time. They both rise and fall with similar gradients. This is in correlation to the trend observed for day one and three.

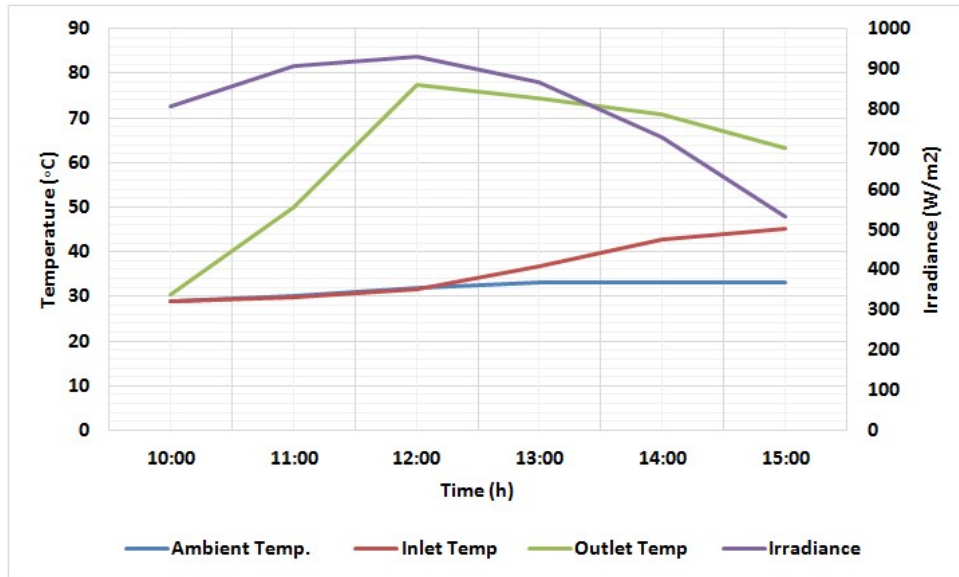


**Figure 2: (a) Temperature against irradiance for day four**

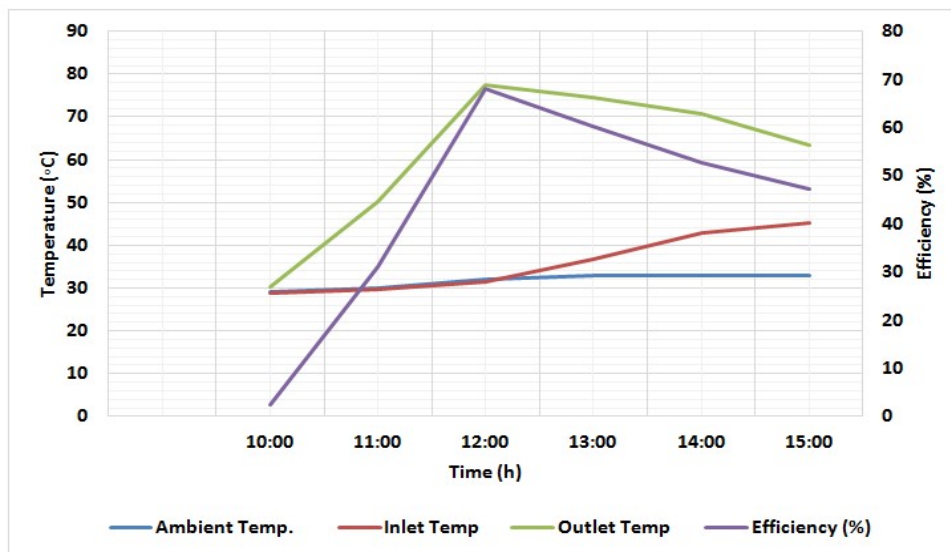


**Figure 2: (b) Temperature against efficiency for day four**

**Table 2: Readings for the fifth day of experiment**

| Time (h) | Ambient Temp. (°C) | Inlet Temp (°C) | Outlet Temp (°C) | Irradiance W/m <sup>2</sup> | Efficiency (%) |
|----------|--------------------|-----------------|------------------|-----------------------------|----------------|
| 10:00    | 29.00              | 30.10           | 31.50            | 824                         | 2.35           |
| 11:00    | 29.00              | 34.30           | 53.10            | 903                         | 28.76          |
| 12:00    | 31.00              | 37.80           | 64.50            | 903                         | 58.45          |
| 13:00    | 32.00              | 43.60           | 64.50            | 823                         | 35.09          |
| 14:00    | 32.00              | 46.50           | 60.30            | 671                         | 28.41          |
| 15:00    | 32.00              | 46.70           | 55.60            | 460                         | 26.73          |

For the fifth day, Figure 3(a) shows that the irradiance rises between 10am and 11am, then remained constant till 12pm after which it gradually falls. This trend is not in line to those observed on the previous days of the testing. The outlet temperature peaks at 12pm similar to day four. Figure 3(b) shows that the efficiency and the outlet temperature both peak at the same time and have similar trend lines. This shows a correlation with the results from the fourth day.

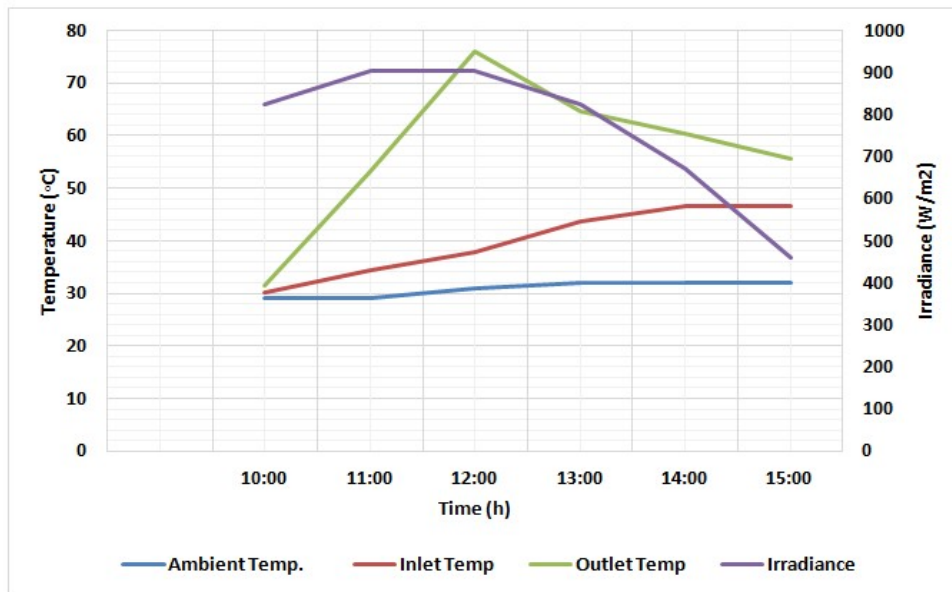


**Figure 3: (a) Temperature against irradiance for day five**

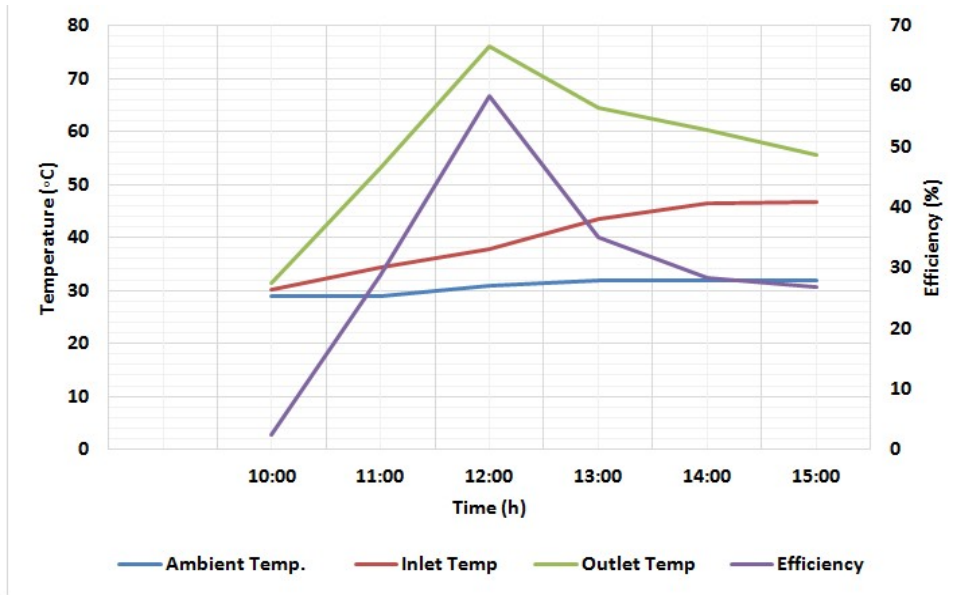


**Figure 3(b) Temperature against efficiency for day five**

**Table 3: Readings for the sixth day of experiment**

| Time (h) | Ambient Temp. (°C) | Inlet Temp (°C) | Outlet Temp (°C) | Irradiance W/m <sup>2</sup> | Efficiency (%) |
|----------|--------------------|-----------------|------------------|-----------------------------|----------------|
| 10:00    | 30.00              | 30.50           | 33.20            | 816                         | 4.57           |
| 11:00    | 30.00              | 31.70           | 59.80            | 916                         | 42.38          |
| 12:00    | 32.00              | 34.20           | 79.30            | 940                         | 66.29          |
| 13:00    | 33.00              | 39.80           | 73.50            | 884                         | 52.67          |
| 14:00    | 34.00              | 40.10           | 65.70            | 750                         | 47.16          |
| 15:00    | 34.00              | 43.40           | 60.20            | 551                         | 42.12          |

From Figure 4(a), The outlet temperature reaches a peak of 79.3°C at noon. This is the highest observed compared to the previous days of testing. The irradiance levels also peak at noon, following with the trend from day four and five. For Figure 4(b), the relationship between the efficiency and the outlet temperature is similar to that of day four and five. The maximum efficiency observed on the last day of testing was 66.29%.

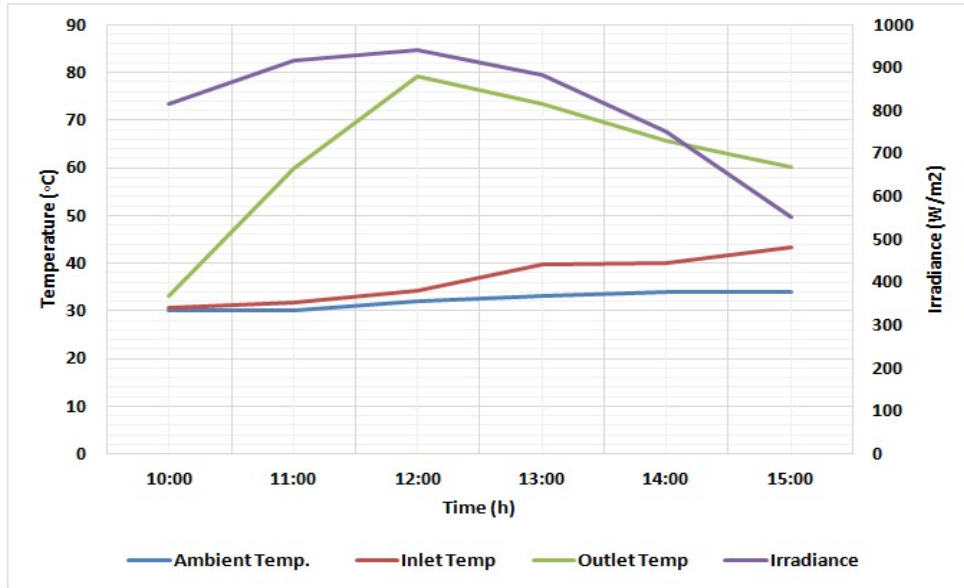


Figure 4(a) Temperature against irradiance for day six

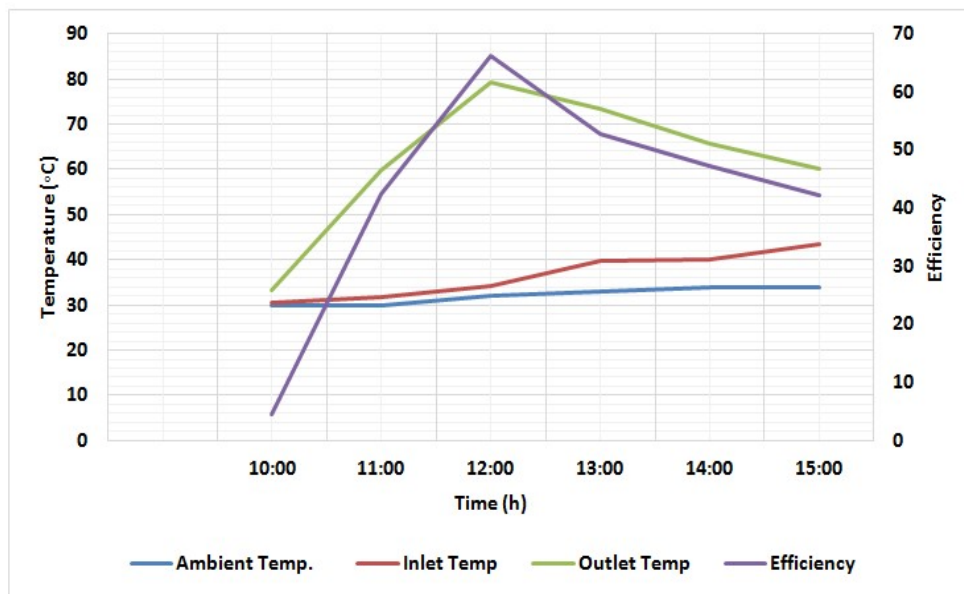
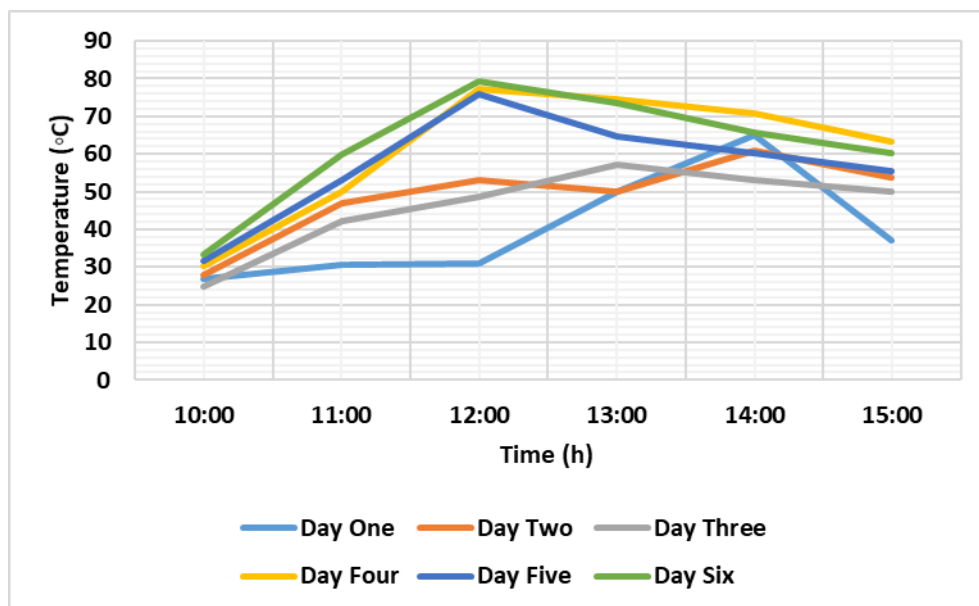


Figure 4(b) Temperature against efficiency for day six

**Table 4: Outlet temperature for the six days of testing**

| Time (h) | Day One | Day Two | Day Three | Day Four | Day Five | Day Six |
|----------|---------|---------|-----------|----------|----------|---------|
| 10:00    | 27.00   | 28.00   | 24.80     | 30.30    | 31.50    | 33.20   |
| 11:00    | 30.50   | 46.80   | 42.10     | 50.10    | 53.10    | 59.80   |
| 12:00    | 31.10   | 53.00   | 48.50     | 77.40    | 76.00    | 79.30   |
| 13:00    | 50.00   | 50.10   | 57.10     | 74.50    | 64.50    | 73.50   |
| 14:00    | 65.00   | 61.00   | 53.00     | 70.80    | 60.30    | 65.70   |
| 15:00    | 37.00   | 53.80   | 50.10     | 63.30    | 55.60    | 60.20   |

Figure 5 shows a significant difference in the outlet temperatures for day one to three compared to those for day four to six. The testing for day one to three was during the late rainy season while those for day four to six was during the dry season. The peak outlet temperature for day one to three occurred between 1pm and 2pm, while the peak for day four to six occurred at noon. This is an evidence that the system performs better in the dry season.



**Figure 5 Outlet temperature for the six days of testing**

It was shown from the analysis results that the irradiance levels and the output temperature are closely related. For the first three days of the testing during the late raining season, an outlet temperature of 65 °C was the highest temperature observed. However, for the last three days of the testing during the dry season, the maximum outlet temperature observed was 79.3 °C. This clearly shows that the system performs better during the dry season. The system was designed with a desired output temperature of 70 °C and the collector area used was 0.76 m<sup>2</sup> obtained during the development process. The total volume of water heated up was 36 litres.

From the work of [9], they designed a solar water heater to provide 75 litres of water at 60 °C daily. From their design, the collector area required was 1.464 m<sup>2</sup>. However, they used an area of 2.3m<sup>2</sup> during the construction of their system and obtained a maximum output of 76 °C. Comparing the two results, shows that although used a larger collector area, their peak outlet temperature was slightly lower than the peak value obtained in this work. This shows that using a larger collector area would not necessarily improve performance; the irradiance available at the system site also plays a significant role on the system performance.

The highest irradiance level of 940 W/m<sup>2</sup> was observed on day six, the highest outlet temperature of 79.3 °C was also observed on the same day and at the same time. The highest raise in outlet temperature was observed on day four with a temperature rise of 47.1 °C between ten am and noon. It is noteworthy that day three had the lowest irradiance levels. The highest efficiency gotten from the system was 68.19 % on day four.

## 6. CONCLUSION

In this work, the design and construction of a 36-litre capacity portable solar water heater has been carried out using relevant equations to obtain the required dimensions of the major components of the system. The materials for the components were selected with consideration to the design calculations, machinability, market availability and cost of the materials. The system was tested, and the following results were observed. From the first three days of testing during the late raining season, the highest outlet temperature recorded was 65°C. For the last three days of testing during the dry season, the highest outlet temperature recorded was 79.3 °C. This difference clearly shows that the system performs better during the dry season when the irradiance levels are higher.

The highest irradiance recorded was 940 W/m<sup>2</sup> on the sixth day of testing while the highest efficiency recorded from the system was 68.19%. It was also noted during the analysis that using a larger collector area would not necessarily improve the system performance; the irradiance available at the system site also plays a significant role on the system performance. Due to time and financial constraints, the followings are recommended as future modifications to enhance the system effectiveness and performance: (i) Installation of a sensor to determine water level and control flow rate, and (ii) Installation of a flow meter to easily measure the flow rate of working fluid.

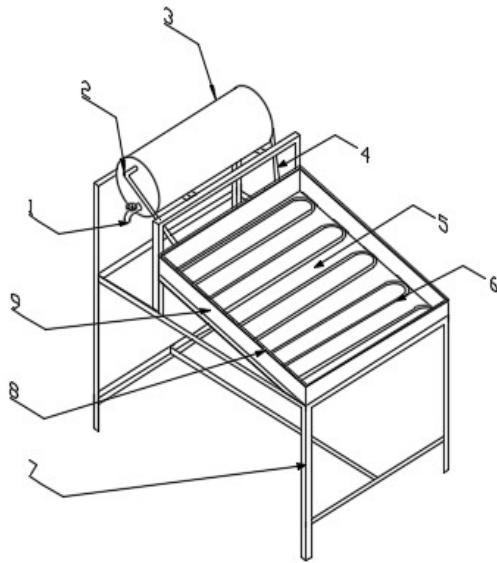
## REFERENCES

1. Swapnil R. Mane and Rajesh V. Kale 2021. IOP Conference Series: Materials Science and Engineering **1091** 012021
2. Abdunnabi, M., Rohuma, I., Endya, E., & Belal, E. (2018). *Review on solar water heating in Libya*.[https://www.researchgate.net/publication/329845152\\_Review\\_on\\_solar\\_water\\_heating\\_in\\_Libya/figures?lo=1](https://www.researchgate.net/publication/329845152_Review_on_solar_water_heating_in_Libya/figures?lo=1).
3. Layton, J. (2009). *Solar Water Heating Systems | HowStuffWorks*.  
<https://science.howstuffworks.com/environmental/green-tech/sustainable/solar-water-heater1.htm>
4. Rikoto, I. I., & Garba, M. M. (2015). *Design Construction and Installation of 250-Liter Capacity Solar Water Heating System at Danjawa Renewable Energy Model Village*. 4, 39–44. [www.tijournals.com](http://www.tijournals.com)
5. Ogie, N. A., Oghogho, I., & Jesumirewhe, J. (2013). Design and Construction of a Solar Water Heater Based on the Thermosyphon Principle. *Journal of Fundamentals of Renewable Energy and Applications*, 3, 1–8. <https://doi.org/10.4303/jfrea/235592>

6. Osinowo, A. A., Okogbue, E. C., Ogungbenro, S. B., & Fashanu, O. (2015). Analysis of Global Solar Irradiance over Climatic Zones in Nigeria for Solar Energy Applications. *Journal of Solar Energy*, 2015, 1–9. <https://doi.org/10.1155/2015/819307>
7. Lilian, I. N., Daniel, O., & Joseph., O. (2018). Modeling the Solar Radiation Parameter over Abuja using Neural Networks. *Undefined*.
8. Bracamonte, J., Parada, J., Dimas, J., and Baritto, M. “Effect of the collector tilt angle on thermal efficiency and stratification of passive water in glass evacuated tube solar water heater,” *Appl. Energy*, vol. 155, pp. 648–659, Oct. 2015, doi: 10.1016/j.apenergy.2015.06.00
9. Ekpo, J., & Enyinna, P. (2017). Design and Construction of a Solar Water Heater for Environmental Sustainability. *British Journal of Applied Science & Technology*, 20(3), 1–15. <https://doi.org/10.9734/bjast/2017/31820>

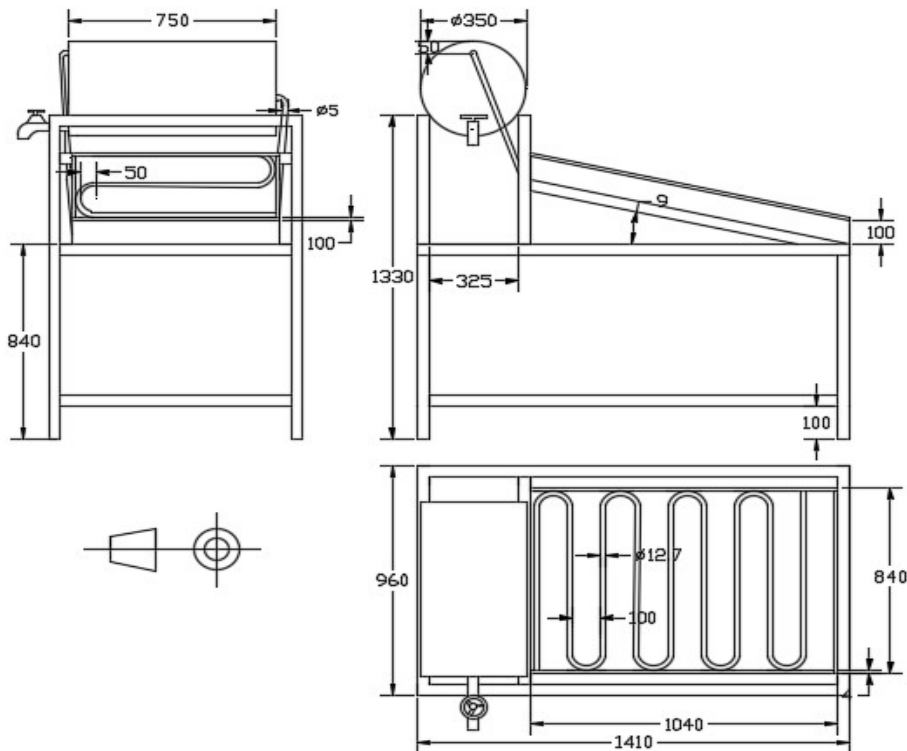
### Appendix I

### Engineering Drawing of the Portable Solar Water Heater



| S/N | Component         | Material                                  |
|-----|-------------------|---|
| 1   | Discharge Tape    | Alluminium Alloy                          |
| 2   | Inlet Flow Pipe   | Copper                                    |
| 3   | Storage Tank      | Stainless Steel and Fibre glass Insulator |
| 4   | Out Flow Pipe     | Copper                                    |
| 5   | Absorber Plate    | Alluminium Plate and Black Paint          |
| 6   | Flow Channel      | Copper Pipe and Black Paint               |
| 7   | Supporting Frame  | Angle Metal (4mm x 12mm)                  |
| 8   | Transparent Cover | Glass (4mm Thick)                         |
| 9   | Collector Casing  | Mild Steel (2mm thick)                    |

**All Components Dimensions in mm**



**Appendix II**  
**The Artefact of the Portable Solar Water Heater During Testing**

